published in Journal of Electroanalytical Chemistry 756 (2015) 207–211

Free Zn^{2+} determination in systems with Zn-Glutathione

Mireia Lao[a], Angela Dago[b], Nuria Serrano[b], Encarna Companys[a], Jaume Puy[a] and Josep Galceran[a]*

[a] Departament de Química, Universitat de Lleida and AGROTECNIO, Rovira Roure 191, 25198 Lleida, Spain
[b] Departament de Química Analítica. Universitat de Barcelona, Martí i Franqués 1, 08028 Barcelona
* corresponding author: galceran@quimica.udl.cat

Abstract

Zn-Glutathione speciation was studied applying the electrochemical technique AGNES (Absence of Gradients and Nernstian Equilibrium Stripping) to determine the free zinc concentration. In titrations varying either pH, total concentration of gluthatione ($c_{T,GSH}$) or total concentration of Zn ($c_{T,Zn}$), free Zn concentrations determined with AGNES were compared with the values predicted from previously reported complexation constants. The speciation of Zn was studied in a real sample of root extracts of *Hordeum vulgare* where the $c_{T,Zn}$ had been determined by ICP-MS and $c_{T,GSH}$ by HPLC. The free [Zn^{2+}] was measured with AGNES using a special device where a mixture of N_2/CO_2 saturated in milliQ water controls the pH and avoids the evaporation of the sample. The lower free zinc concentration determined with AGNES, in comparison with the predicted one assuming the literature complexation constants and taking into account only the presence of Zn and GSH, indicates that it is necessary to include more ligands apart from GSH (as other phytochelatins) in the speciation model.

Keywords:
Absence of Gradients and Nernstian Equilibrium Stripping; Speciation techniques; glutathione; Zinc complexes; Environmental analysis

published in Journal of Electroanalytical Chemistry 756 (2015) 207–211

1. Introduction

The tripeptide Glutathione (GSH) with the sequence γ-Glu-Cys-Gly is widely present in living systems and it is usually the most abundant intracellular nonprotein thiol. GSH has two peptide bonds, two carboxylic acid groups, one amino group and one thiol group. Due to the affinity of the thiol group for heavy metals, GSH plays an important role in the complexation and elimination of the toxic metals from the organisms [1]. Furthermore, the structure of GSH is directly linked to that of phytochelatins, which are thiol-rich peptides synthesized enzymatically by plants in response to an excessive uptake of certain heavy metal ions, such as Cd(II), Pb(II), Zn(II), Ag(I), Hg(II), Cu(I) [2-8]. Therefore, the study of the complexation of heavy metal ions by GSH is of great interest as a model system for the binding of metal ions by larger thiol-containing peptides and proteins [9,10].

Heavy metals arrive to natural waters from industrial wastes, mining activities, fertilizers, paints, and atmospheric depositions. As heavy metals cannot be degraded they may enter the body in food, water, air or by absorption through the skin. Once in the body, they compete with and displace essential elements such as Zn, Cu, Mg and Ca, and interfere with organ system functions. Particularly, Zn deficiency is considered as a wide-spread malnutrition problem that affects the growth of children [11], but at elevated levels Zn becomes toxic to terrestrial and aquatic organisms. Heavy metals are especially dangerous because they tend to bioaccumulate, e.g. they accumulate in the soft tissues [12]. Nevertheless, it has to be taken into consideration that the bioavailability of heavy metals to organisms depends mostly on the free metal ion concentration (which is directly related to activity) [13-15]. This is why the development of suitable analytical techniques for measuring free metal ion concentrations at trace levels in natural samples is required[16]. In particular, for the direct measurement of free Zn(II) concentration, the voltammetric technique Absence of

Gradients and Nernstian Equilibrium Stripping (AGNES) has been proved as a reliable, low cost and easy to interpret electrochemical technique [17,18]. Moreover, AGNES has been successfully applied to synthetic and natural samples like sea [19] and river water [20], soil extracts [20] and nanoparticle dispersions [21].

The complexation of Zn(II) by GSH has been extensively studied by electroanalytical techniques such as differential pulse polarography (DPP) or constant current chronopotentiometric stripping analysis using adsorptive accumulation (AdSCP) on mercury electrode assisted by multivariate curve resolution method by alternating least-squares (MCR-ALS) [22]. However, the determination of free Zn(II) concentration in plant extracts has not been investigated yet.

The aim of this work is to study the Zn-GSH system in a natural sample with AGNES. As a previous step, the complexation of Zn with GSH was analyzed using this voltammetric technique in synthetic systems at various pH values and different total ligand and metal concentrations to compare with existing complexation models [23], [24] and [25]. Subsequently, free Zn concentration has also been measured with AGNES in *Hordeum vulgare* root extracts.

2. Material and Methods

2.1 Equipment and Reagents

The voltammetric measurements were done using a μ-AUTOLAB type III potentiostat attached to a Metrohm 663 VA Stand and to a computer by means of NOVA 1.10 (Eco Chemie) package software. The Metrohm Hanging Mercury Drop Electrode (HMDE) was the working electrode. The smallest drop (drop 1, which according to the catalogue corresponds to a radius $r_0=1.41\times10^{-4}$ m) was chosen to perform AGNES measurements and the largest drop (drop 3 which corresponds to an $r_0=2.03\times10^{-4}$ m) to perform Differential Pulse Polarograms (DPP). The auxiliary electrode was a glassy carbon

electrode and the reference electrode was Ag|AgCl (3 mol L^{-1}) KCl, encased in a 0.1 mol L^{-1} KNO_3 jacket.

The total metal concentration of the natural samples was determined by ICP-MS, 7700x from Agilent (Santa Clara, USA).

Zn solutions were prepared from Merck (Darmstadt, Germany) 1000 mg L^{-1} standard solutions. Potassium nitrate was used as supporting electrolyte and prepared from solid KNO_3 TraceSelect (Sigma Aldrich, St. Louis, MO, USA). GSH solutions were prepared from EMPROVE* blo Glutathione (reduced) from Merck. To keep the pH fixed at 7.5 and 8.0, the buffer 4-(2-Hydroxyethyl)-1-piperazinepropanesulfonic acid (EPPS) from Sigma Aldrich (≥ 99.5%) was used. In all experiments, ultrapure water (Synnergy UV Millipore) was used.

To prepare the Hoagland solution (nutrient solution) for culturing plants, $Ca(NO_3)_2$, $Fe(NO_3)_3 \cdot 9\ H_2O$ and $CuSO_4 \cdot 5\ H_2O$ from Probus (Badalona, Spain), KNO_3, $MnSO_4 \cdot H_2O$ and $ZnCl_2$ from Merck (Darmstadt, Germany) and $Mg(NO_3)_2 \cdot 6\ H_2O$, KH_2PO_4, H_3BO_3 and $Mo_7O_{24}(NH_4)_6$ from Panreac (Barcelona, Spain), were used. Plants were stressed adding $Zn(NO_3)_2 \cdot 4\ H_2O$ from Merck to the nutrient solution.

An Agilent (Santa Clara, CA, USA) 1100 chromatographic system was used for GSH determination in plant root extracts. The system was equipped with a quaternary pump, a Rheodyne 7725i 20 μL loop manual injector (Rohnert Park, CA, USA), a vacuum degasser and a handheld control module. An Ascentis C18 5 μm particle size analytical column measuring 25 cm x 4.6 mm was provided by Supelco (Bellefonte, PA, USA).

The electrochemical detector (ED) consisted of a CC-5C flow cell BASi (West Lafayette, IN, USA), with a three electrode system: a glassy carbon working electrode (BASi), a stainless steel auxiliary electrode and an Ag/AgCl (NaCl 3 mol L^{-1}) reference electrode. The separation between the working and the auxiliary electrodes was

performed by a gasket whose thickness was 0.005 inches that creates the cell volume. The system was connected to an Autolab PGSTAT 12 potentiostat (Eco Chemie, Utrecht, the Netherlands). GPES software version 4.9.007 (Eco Chemie) was used for potentiostatic control and data acquisition.

To prepare the mobile phase for GSH determination by HPLC, trifluoroacetic acid (TFA) provided by Sigma-Aldrich (St. Louis, MO, USA) and acetonitrile from Merck were used.

2.2 Sample preparation

Barley (*Hordeum vulgare* cv. Graphic) seedlings were cultivated hydroponically using Hoagland solution adjusted to pH 6 (in the middle of the recommended range 5.5-6.5). The nutrient solution (Hoagland solution) contained 268 mg L^{-1} of N, 235 mg L^{-1} of K, 200 mg L^{-1} of Ca, 31 mg L^{-1} of P, 0.30 mg L^{-1} of S and 48.6 mg L^{-1} of Mg as macronutrients, and 0.5 mg L^{-1} of B, 2.50 mg L^{-1} of Fe, 0.5 mg L^{-1} of Mn, 0.05 mg L^{-1} of Zn, 0.02 mg L^{-1} of Cu and 0.01 mg L^{-1} of Mo as micronutrients. Seeds were placed on top of a mesh situated over a plastic container filled with nutrient solution, so that the seeds were slightly in contact with the nutrient solution. Five days after seeds were sowed, the nutrient solutions were changed for Hoagland solutions where Zn^{2+} had been added at a concentration of 500 µmol L^{-1}.

Three pots with 20 seeds per pot were considered. Barley roots were collected after 9 days of metal treatment. Plants were cleaned first with 0.1 mol L^{-1} EDTA solution and then with milliQ water, frozen at once with liquid nitrogen to disrupt cell walls and stored at -80ºC. Subsequently, samples were ground separately in liquid nitrogen.

For the extraction of GSH, 120 mg of sample fresh weight (thawed at room temperature) were mixed with 12 mL of ultrapure filtered water for 1 hour in a rotatory

horizontal stirrer from SBS (Barcelona, Spain). Prior to analysis, samples were filtrated through 0.45 μm nylon filter discs by Osmonics (Minnetonka, MN, USA). The filtered solution was stored at -25ºC.

2.3 Free Zinc determination

2.3.1 AGNES principles

Being a stripping technique, AGNES consists of two different stages: accumulation and quantification [17]. In the simplest implementation (AGNES-1P) of the first stage, the metal in solution (Zn^{2+}, in this work) is reduced by applying a negative potential (E_1) for a long enough time (t_1), reaching, by the end of the stage, Nernstian equilibrium and flat concentration profiles of Zn^{2+} and Zn^0.

The gain (Y) is the desired ratio between the metal concentrations at both sides of the electrode surface:

$$Y = \frac{\left[\mathrm{Zn}^0\right]}{\left[\mathrm{Zn}^{2+}\right]} = \exp\left[-\frac{nF}{RT}\left(E_1 - E^{0'}\right)\right] \quad (1)$$

where n is the number of electrons involved in the faradaic process, F the Faraday constant, R the gas constant, T the temperature, E_1 the applied deposition potential and $E^{0'}$ the standard formal potential.

Experimentally, the potential (E_1) needed to reach the desired gain (Y) can be computed from the peak potential of a differential pulse polarogram (DPP):

$$Y = \sqrt{\frac{D_{\mathrm{Zn}^{2+}}}{D_{\mathrm{Zn}^0}}}\exp\left[-\frac{nF}{RT}\left(E_1 - E_{\mathrm{peak}} - \frac{\Delta E}{2}\right)\right] \quad (2)$$

where E_{peak} is the potential of the maximum obtained in a I vs E DPP-plot.

In the second stage, a re-oxidation potential (E_2) is applied to quantify the metal amalgamated in the mercury.

If the analytical response for quantification is the current under diffusion-limited conditions, the free metal ion concentration can be computed with the proportionality factor η:

$$I = Y\eta\left[\mathrm{Zn}^{2+}\right] \quad (3)$$

If the analytical response is the charge, the combination of Nernst and Faraday laws prescribe [18,26]

$$Q = Y\eta_{\mathrm{Q}}\left[\mathrm{Zn}^{2+}\right] \quad (4)$$

When the free metal ion concentration in the sample is at trace level, one needs larger gains and the deposition time (t_1) might be too long. Then, the first stage of AGNES is split into two sub-stages (variant AGNES-2P): i) a sub-stage applying a very negative potential under diffusion limited conditions $E_{1,a}$ during $t_{1,a}$ ii) followed by another sub-stage applying a potential $E_{1,b}$ corresponding to the desired gain (Y) during $t_{1,b}$ seconds [27,28].

2.3.2 Special device to control the evaporation and fixing the pH

Voltammetric techniques usually work under nitrogen atmosphere, as the presence of oxygen interferes in the response. As this nitrogen flux can change the nature of the sample (removing gases such as CO_2 and therefore breaking the equilibrium state between the dissolved gas, dissolved CO_3^{2-} and the precipitated carbonates), a specific purging system (with a mixture of N_2/O_2 [29-31]) has been used for the measurements in the root extracts of *Hordeum vulgare*.

As seen in figure 1, when the measurement is running, the tube a (which in the standard stand is used to provide the nitrogen to the cell), goes through a T-shaped teflon key labelled as B to a glass bottle filled with water (c1 tube). At the same time, the tube d

transports the CO_2 to the same bottle. Both gases bubble into the milliQ water (glass bottle E) to get them saturated and the resulting gas mixture exits via tube (f) and goes through the other T-shaped Teflon key labelled as G to the cell I (via tube h). But, at the moment of the drop formation, the keys' position is switched to have the necessary pressure, see inset in figure 1).

2.4 GSH determination

HPLC with amperometric detection was used for GSH determination in plant root extracts. The mobile phase consisted of 0.1% trifluoroacetic acid (TFA) in ultrapure filtered water, pH=2.00, and 0.1% TFA in acetonitrile. Gradient separation was achieved at ambient temperature with a gradient profile as described in [9]. The flow rate was 1.2 mL min^{-1}.

For preparing the surface of the working electrode, mechanical polishing was daily done using a suspension of 0.3 μm alumina particles from Metrohm (Herisau, Switzerland), followed by ethanol rinsing and sonication for 5 min in ethanol and 5 min in ultrapure filtered water. The optimised potential for the working electrode was 1.2 V.

3. Results and discussion

3.1 Free zinc determination in synthetic solutions of Zn-GSH

Literature values from [23], [24] and [25] for the thermodynamic constants of the different species of GSH, extrapolated to zero ionic strength by using Davies correction, are shown in Table 1. Four VMINTEQ database sets (available as 8 files in Supporting Information) have been prepared to compute speciation when needed for the different models labelled as follows: DiazCruz I (considering two complexes with just one metal

ion), DiazCruz II (contemplating one complex with one metal ion and another with two metal ions), Ferretti (8 complexes) and Krezel (6 complexes). For the models of DiazCruz [25], the two values (arising from two mathematical treatments) given by the authors in their Table 2 have been averaged before extrapolation at infinite dilution.

3.1.1 Zn-GSH speciation varying the pH

The evolution of free Zn concentration in a solution with fixed amounts of Zn and GSH along a pH change (via addition of potassium hydroxide) has been followed. Free zinc concentration determined by AGNES is compared with the predicted values from VMinteq for the 4 considered speciation models (see Figure 2). Below pH 4.5, practically all Zn is in its free form. For higher pH values, the competition of proton for GSH sites is less important and the free zinc concentration decreases. The theoretical results corresponding to both models from DiazCruz are far from the experimental results. It is not surprising, because both models just consider two complex species: ZnG^{-} and ZnG_2^{4-} (model I) or ZnG_2^{4-} and $Zn_2G_2^{4-}$ (model II). Moreover the use of borate buffer, whose complexation was not taken into account, might also be behind the mismatch.

The models of Ferretti and Krezel are closer to the experimental results of this work, especially in the case of Krezel model which practically agrees with AGNES (Figure 2). In terms of the various complex Zn-GSH species, both models are quite similar in the set of assumed complexes and the values of the stability constants. In fact there are just two more species in the model of Ferretti ($Zn_2G_2H_{-1}^{3-}$ and $Zn_2G_2H_{-2}^{4-}$, whose concentrations are practically negligible in the probed conditions as those species appear from pH 8 on) than in Krezel model.

For the specific concentration conditions (total Zn concentration, $c_{T,Zn}$=1.6×10^{-3} mol L^{-1} and total GSH concentration, $c_{T,GSH}$=2.9×10^{-3} mol L^{-1}) used in the figure, the discrepancies between the free Zn concentrations predicted by Krezel's and Ferretti's models are maximum in the pH region 7-8. These discrepancies between Ferretti's and Krezel's models can be visualized (see Figure 3) via the percentage of difference between the fractions of Zn, x_j (concentration of the species over the total concentration of Zn), predicted by both models for a given species. The main difference involves species ZnG_2^{4-} and $ZnG_2H_2^{2-}$. The first specie (ZnG_2^{4-}) is more abundant in Krezel's model (where it reaches 0.2% of the total Zn at pH 7 and 4.9% at pH 8) than in Ferretti's model. The second specie ($ZnG_2H_2^{2-}$) is more abundant in Ferreti's model (28.5% of the total Zn at pH 7 and 11.6% at pH 8) than in Krezel's model. Details on the distribution of species can be seen comparing figures SI-1 and SI-2.

3.1.2 Zn-GSH titration fixing $c_{T,Zn}$ and pH while varying $c_{T,GSH}$

The suitability of the models has also been studied via two titrations where pH was fixed at 7.5 and 8. The range of $c_{T,Zn}$ has also been selected in the concentration region in the μmol L^{-1} range where the difference between models is larger (for resulting free concentrations above nanomolar). To fix the pH, several buffer solutions as borate, tris(hydroxymethyl)aminomethane (TRIS) and EPPS were tested. EPPS was chosen because DPP experiments indicated complexation of Zn by borate and TRIS, but not by EPPS.

In Figure 4, at lower total Zn concentration, it is again observed that the predictions of [Zn^{2+}] in DiazCruz models are far from the experimental results in comparison with Ferretti and Krezel models. For these conditions, the most accurate model seems to be

Ferretti's. A similar behaviour is seen in figure SI-3, now at a total Zn concentration of 0.1 mmol L^{-1}. We considered whether the differences in the predictions of free Zn between Ferretti and Krezel models could be due to the slightly different protonation constants. To check this, we forced the protonation GSH constants of Krezel into the model of Ferretti, but there was no agreement neither with the experimental data nor with the predictions of Krezel's model. The same happened when introducing the protonation GSH constants of Ferretti into Krezel's model.

3.2 Zn speciation in root extracts of *Hordeum vulgare*

The analysis of GSH in root extracts of *Hordeum vulgare* plants was performed by HPLC with amperometric detection. The quantification was done by external calibration curve with high linearity (determination coefficient r^2=0.9998) with standards ranging from 1 to 10 µmol L^{-1}. The obtained limits of detection and quantification were 1.57×10^{-7} and 5.23×10^{-7} mol L^{-1}, respectively. Three independent replicates (labelled 1, 2 and 3) were analysed obtaining an average concentration of GSH of 1.327 ± 0.003 µmol L^{-1}.

The total Zinc concentration in these three samples was determined by ICP-MS. As seen in Table 2, the total concentration is around 10 µmol L^{-1}, leading to a sufficiently high free zinc concentration as to be determined with AGNES-1P and moderate gains.

To ensure the reliability of the results, all measurements were done twice and with two different gains (*Y*=20 and *Y*=50), taking as AGNES response both the intensity (AGNES-I) and the charge (AGNES-Q). The used deposition times were 350 and 500s for *Y*=50 and 175 and 250s for *Y*=20 which clearly satisfy or overpass the usual rule [32]:

$$t_1 - t_w = 7\mathrm{Y} \qquad (5)$$

We work with two different deposition times (for each gain) to ensure that AGNES equilibrium was reached.

All replicates for each sample showed a good agreement between them. The reproducibility between samples is also good (see Table 2).

The experimentally determined free zinc concentration (just around 2% of the total zinc) is lower than the theoretically expected just taking into account GSH complexation following the models of Ferretti and Krezel by a factor around 50. This means that in the samples there are other ligands apart from GSH which are complexing most of the metal. This could be explained from the complexation of Zn with phytochelatins (synthesized by its precursor GSH), as observed with other metals and metalloids such as Hg, Cd or As [9,10], triggered by the large level of the stressor Zn in the hydroponic medium.

4. Conclusions

AGNES can be used to assess the accuracy in the predictions of free Zn concentrations between competing complexation models by comparing the determined free zinc concentration in different titrations with the theoretical one obtained with a speciation program (such as VMinteq). In the specific studied case, four different models from the literature with the complexation constants of the system Zn- GSH were compared.

When pH was changed for $c_{T,GSH}$ in the mmol L^{-1} range, Krezel model appears as the most suitable one, closely followed by Ferretti's, showing the largest difference in the pH region 7-8. The main discrepancy is different relevance for particular species that each model present (ZnG_2^{4-} in the case of Krezel and $ZnG_2H_2^{2-}$ for Ferretti). But, when this specific pH region was studied in the μmol L^{-1} range, the opposite situation happened (the most suitable model was Ferretti). Taking into consideration the possible

experimental uncertainty, a clear prioritisation of these two models cannot be done. So, when the root extracts of *Hordeum vulgare* were analyzed, the experimental results were compared with both models (even if the difference between the predictions is smaller than the experimental error). In the extracts almost all Zn is complexed (98%). On the other hand, the experimental free zinc concentration is 50 times lower than the theoretical one. So, the free Zn concentration is not mostly regulated just by GSH, but it is necessary to consider a more complex scheme including other ligands (such as different types of phytochelatins), as observed in the case of other metals such as Cd or Hg.

Acknowledgements

The authors gratefully acknowledge support of this research by the Spanish Ministry Spanish Ministry of Education and Science (Projects CTQ2009-07831, CTM2012-39183, CTQ2012-32863 and CTM2013-48967) and by the "Comissionat d'Universitats i Recerca de la Generalitat de Catalunya" (2014SGR269 and 2014SGR1132). ML acknowledges a FPI grant from the Spanish Ministry.

References

[1] D.Dolphin, O.Avramovic, R.Poulson, Glutathione. Chemical, Biochemical and Medical Aspects, New York, 1989.

[2] W.E.Rauser, Plan. Physiol. 109 (1995) 1141.

[3] E.Grill, E.L.Winnacker, M.H.Zenk, Science 230 (1985) 674.

[4] E.Grill, E.L.Winnacker, M.H.Zenk, Proceedings of the National Academy of Sciences of the United States of America 84 (1987) 439.

[5] W.E.Rauser, Annual Review of Biochemistry 59 (1990) 61.

[6] B.A.Ahner, N.M.Price, F.M.M.Morel, Proceedings of the National Academy of Sciences of the United States of America 91 (1994) 8433.

[7] M.H.Zenk, Gene 179 (1996) 21.

[8] P.Soudek, S.Petrova, R.Vankova, J.Song, T.Vanek, Chemosphere 104 (2014) 15.

[9] A.Dago, O.Gonzalez-Garcia, C.Arino, J.M.Diaz-Cruz, M.Esteban, Anal. Chim. Acta 695 (2011) 51.

[10] A.Dago, I.Gonzalez, C.Arino, J.M.Diaz-Cruz, M.Esteban, Talanta 118 (2014) 201.

[11] J.G.Penland, Journal of Nutrition 130 (2000) 361S.

[12] E.Lawrence, A.R.W.Jackson, J.M.Jackson, Longman Dictionary of Enviromental Science, Addison Wesley Longman Ltd., London (UK), 1998.

[13] D.R.Parker, J.F.Pedler, Plant Soil 196 (1997) 223.

[14] P.G.C.Campbell, in A. Tessier and D. R. Turner (Eds.), Metal Speciation and Bioavailability in Aquatic Systems, John Wiley & Sons, Chichester (UK), 1995, Chapter 2, p. 45.

[15] Q.Sun, X.R.Wang, S.M.Ding, X.F.Yuan, Chemosphere 60 (2005) 22.

[16] M.Pesavento, G.Alberti, R.Biesuz, Anal. Chim. Acta 631 (2009) 129.

[17] J.Galceran, E.Companys, J.Puy, J.Cecília, J.L.Garcés, J. Electroanal. Chem. 566 (2004) 95.

[18] J.Galceran, M.Lao, C.David, E.Companys, C.Rey-Castro, J.Salvador, J.Puy, J. Electroanal. Chem. 722-723 (2014) 110.

[19] J.Galceran, C.Huidobro, E.Companys, G.Alberti, Talanta 71 (2007) 1795.

[20] D.Chito, L.Weng, J.Galceran, E.Companys, J.Puy, W.H.van Riemsdijk, H.P.van Leeuwen, Sci. Total Envir. 421-422 (2012) 238.

[21] C.David, J.Galceran, C.Rey-Castro, J.Puy, E.Companys, J.Salvador, J.Monné, R.Wallace, A.Vakourov, J. Phys. Chem. C 116 (2012) 11758.

[22] N.Serrano, I.Sestakova, J.M.Diaz-Cruz, C.Arino, J. Electroanal. Chem. 591 (2006) 105.

[23] L.Ferretti, L.Elviri, M.A.Pellinghelli, G.Predieri, M.Tegoni, J. Inorg. Biochem. 101 (2007) 1442.

[24] A.Krezel, J.Wojcik, M.Maciejczyk, W.Bal, Chemical Communications (2003) 704.

[25] M.S.Diaz-Cruz, J.M.Díaz-Cruz, J.Mendieta, R.Tauler, M.Esteban, Anal. Biochem. 279 (2000) 189.

[26] J.Galceran, D.Chito, N.Martinez-Micaelo, E.Companys, C.David, J.Puy, J. Electroanal. Chem. 638 (2010) 131.

[27] E.Companys, J.Cecília, G.Codina, J.Puy, J.Galceran, J. Electroanal. Chem. 576 (2005) 21.

[28] G.Alberti, R.Biesuz, C.Huidobro, E.Companys, J.Puy, J.Galceran, Anal. Chim. Acta 599 (2007) 41.

[29] J.H.Pei, M.L.Tercier-Waeber, J.Buffle, Anal. Chem. 72 (2000) 161.

[30] F.Zavarise, E.Companys, J.Galceran, G.Alberti, A.Profumo, Anal. Bioanal. Chem. 397 (2010) 389.

[31] D.Chito, J.Galceran, E.Companys, J.Puy, J. Agric. Food Chem. 61 (2013) 1051.

[32] D.Chito, J.Galceran, E.Companys, Electroanal. 22 (2010) 2024.

published in Journal of Electroanalytical Chemistry 756 (2015) 207–211

360

TABLE

Table 1. Thermodynamic accumulated constants, log β^{th}, that have been used for DiazCruzI, DiazCruzII [25], Ferretti [23] and Krezel [24] models, where G^{3-} denotes the completely deprotonated glutathione form (i.e. H_3G is GSH).

Reaction	Model			
	DiazCruzI	**DiazCruzII**	**Ferretti**	**Krezel**
$H^+ + G^{3-} \rightleftharpoons HG^{2-}$	10.25	10.25	10.11	10.30
$2H^+ + G^{3-} \rightleftharpoons H_2G^-$	19.37	19.37	19.25	19.46
$3H^+ + G^{3-} \rightleftharpoons H_3G$	23.09	23.09	22.94	23.19
$4H^+ + G^{3-} \rightleftharpoons H_4G^+$	25.17	25.17	25.03	25.32
$Zn^{2+} + G^{3-} \rightleftharpoons ZnG^-$	8.24	-	9.20	9.60
$Zn^{2+} + 2G^{3-} \rightleftharpoons ZnG_2^{4-}$	12.62	12.72	13.03	14.26
$2Zn^{2+} + 2G^{3-} \rightleftharpoons Zn_2G_2^{2-}$	-	21.38	-	-
$Zn^{2+} + G^{3-} + H^+ \rightleftharpoons ZnGH$	-	-	15.71	16.24
$Zn^{2+} + 2G^{3-} + 2H^+ \rightleftharpoons ZnG_2H_2^{2-}$	-	-	31.18	31.65
$Zn^{2+} + 2G^{3-} + H^+ \rightleftharpoons ZnG_2H^{3-}$	-	-	23.22	24.04
$Zn^{2+} + 2G^{3-} \rightleftharpoons ZnG_2H_{-2}^{6-} + 2H^+$	-	-	-10.30	-8.20
$2Zn^{2+} + 2G^{3-} \rightleftharpoons Zn_2G_2H_{-1}^{3-} + H^+$	-	-	11.28	-
$2Zn^{2+} + 2G^{3-} \rightleftharpoons Zn_2G_2H_{-2}^{4-} + 2H^+$	-	-	1.01	-

Table 2. Compilation of [Zn^{2+}] determined by AGNES in root extracts of Hordeum vulgare for two different gains (Y=20 and Y=50). In all cases the experimental results are compared with theoretical predictions by VMinteq using the databases of Ferretti and Krezel

Sample	**pH**	**$c_{T,GSH}$/mol L^{-1}**	**$c_{T,Zn}$ /mol L^{-1} (ICP)**	**[Zn^{2+}]AGNES_I /mol L^{-1}**	**[Zn^{2+}]AGNES_Q /mol L^{-1}**	**[Zn^{2+}]VMinteq /mol L^{-1}**
1	7.30	1.33×10^{-6}	8.58×10^{-5}	1.72×10^{-6} (*Y*=50) 1.70×10^{-6} (*Y*=20)	1.70×10^{-6} (*Y*=50) 1.66×10^{-6} (*Y*=20)	8.28×10^{-5} (Ferretti) 8.27×10^{-5} (Krezel)
2	7.33	1.33×10^{-6}	8.53×10^{-5}	1.70×10^{-6} (*Y*=50) 1.70×10^{-6} (*Y*=20)	1.66×10^{-6} (*Y*=50) 1.63×10^{-6} (*Y*=20)	8.21×10^{-5} (Ferretti) 8.208×10^{-5} (Krezel)
3	7.25	1.32×10^{-6}	9.12×10^{-5}	1.63×10^{-6} (*Y*=50) 1.62×10^{-6} (*Y*=20)	1.64×10^{-6} (*Y*=50) 1.62×10^{-6} (*Y*=20)	8.84×10^{-5} (Ferretti) 8.82×10^{-5} (Krezel)

FIGURES

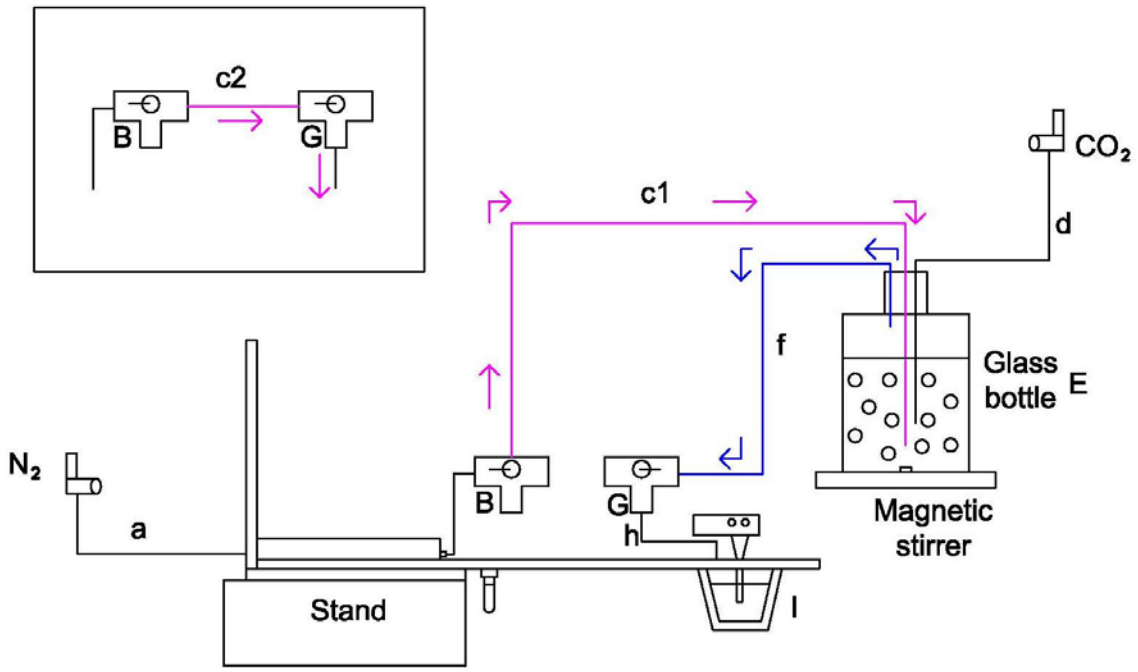

Figure 1: Device used to control the evaporation and to fix the pH. The position of the keys B and G and the arrows in this scheme correspond to the situation during the measurement. For drop formation, it is necessary to change the keys position as shown in the inset.

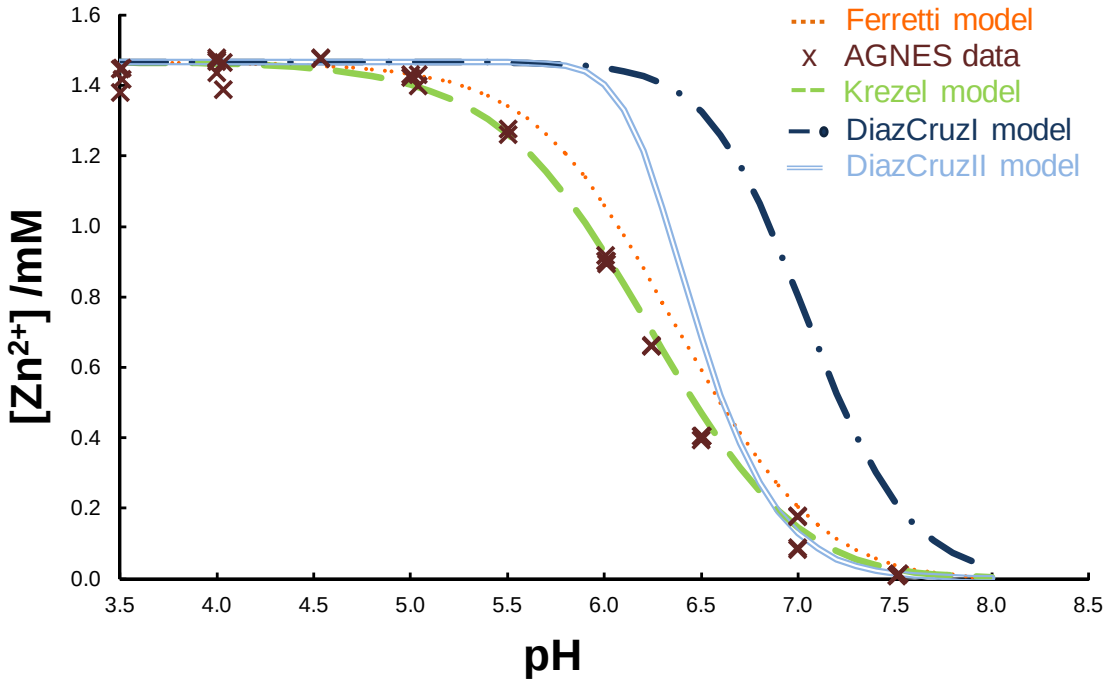

Figure 2: Change of $[Zn^{2+}]$ with pH in a solution where $c_{T,Zn}$= 1.6×10^{-3} mol L^{-1}, $c_{T,GSH}$= 2.9×10^{-3} mol L^{-1} and KNO_3 0.1mol L^{-1}. Brown cross marker corresponds to two replicates of AGNES measurements. Theoretical computations: green dashed line stands for Krezel model, orange dotted line for Ferretti model, dark blue dashed dotted line for DiazCruzI model and double blue line for DiazCruzII model.

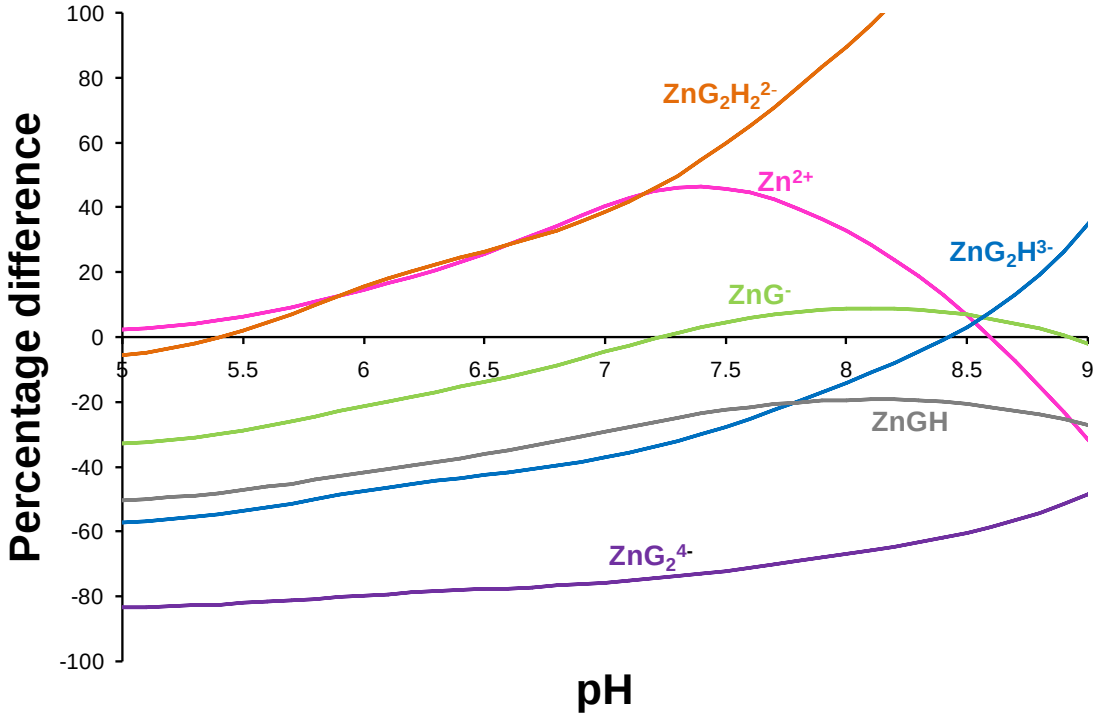

Figure 3: Percentage of difference between Ferretti and Krezel models (expressed as $(\chi_{j;Ferretti} - \chi_{j,Krezel})/ \chi_{j,Krezel})\times100$, where χ_j is the fraction of Zn as species *j*) for main species of Zn in front of pH. Total concentrations: $c_{T,Zn}= 1.6\times10^{-3}$ mol L^{-1}, $c_{T,GSH}= 2.9\times10^{-3}$ mol L^{-1} and KNO_3 0.1 mol L^{-1}.

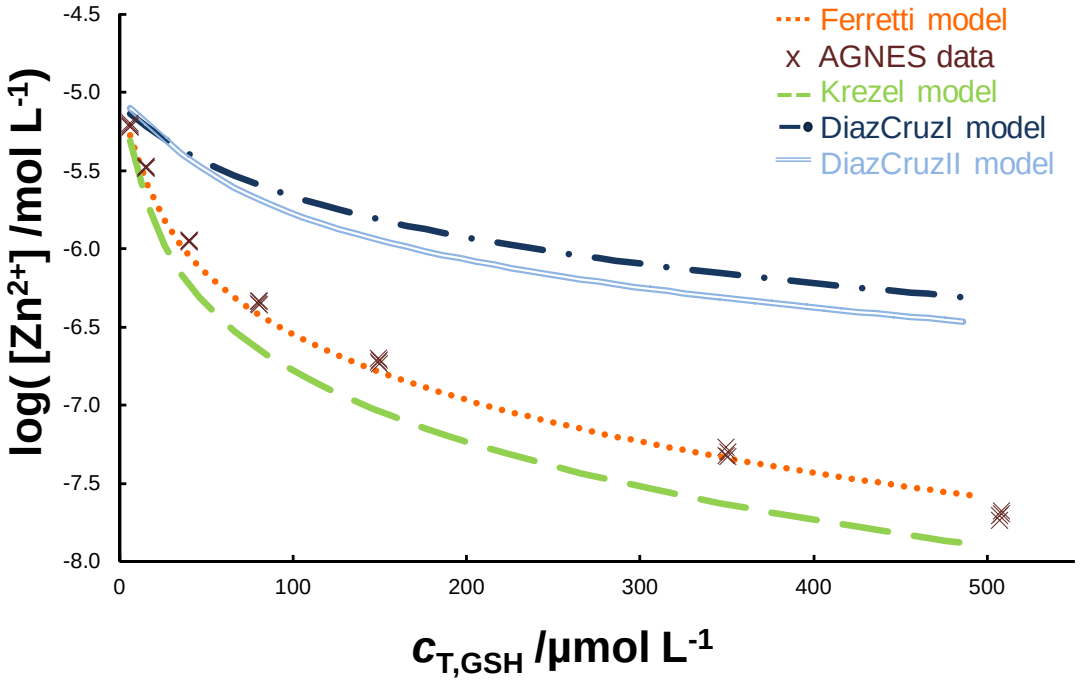

Figure 4: Evolution of $[Zn^{2+}]$ when adding glutathione to a solution where $c_{T,Zn}$= 1×10^{-5} mol L^{-1}, pH 8.00 (10^{-2} mol L^{-1} EPPS) and KNO_3 0.1 mol L^{-1}. Markers and lines as in Fig 2.

published in Journal of Electroanalytical Chemistry 756 (2015) 207–211

SUPORTING INFORMATION

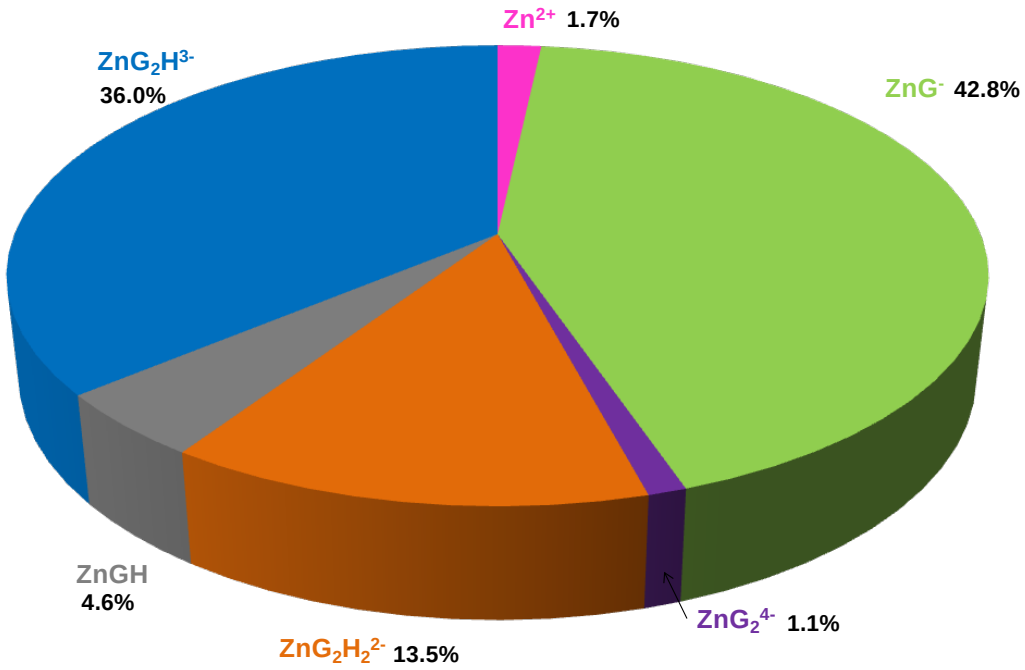

Figure SI-1. Distribution of species according to Krezel's model for the system Zn-GSH with $c_{T,Zn}$= 1.6×10^{-3} mol L^{-1}, $c_{T,GSH}$= 2.9×10^{-3} mol L^{-1}, pH 7.5 and KNO_3 0.1 mol L^{-1} (same concentration conditions as in Figure 3) .

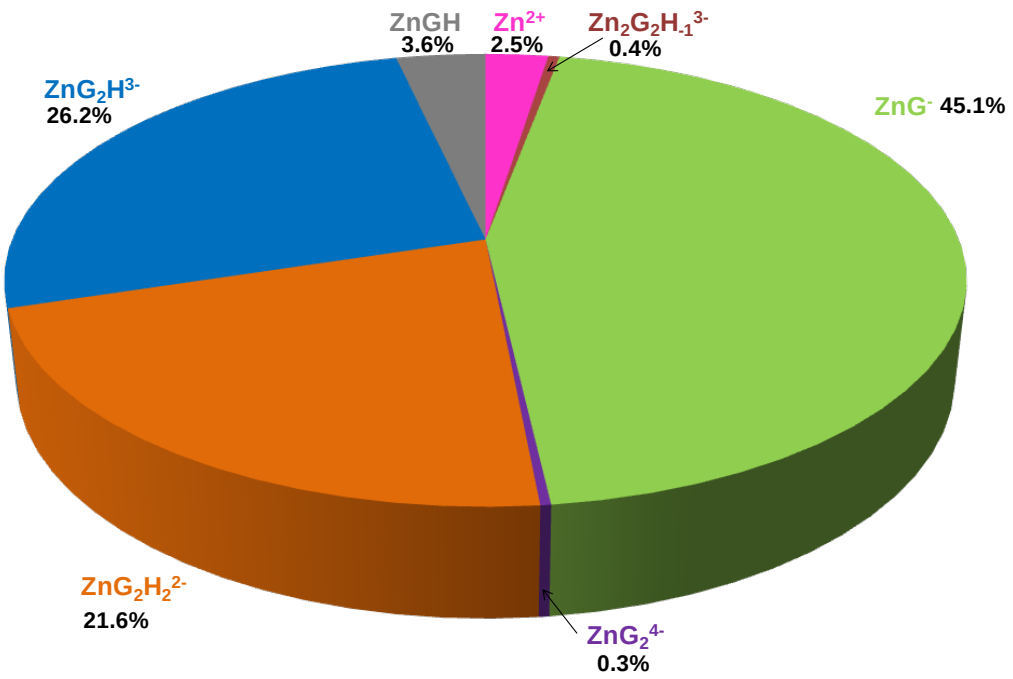

455

456 Figure SI-2. Distribution of species according to Ferretti's model for the system Zn-GSH
457 with $c_{T,Zn}$= 1.6×10^{-3} mol L^{-1}, $c_{T,GSH}$= 2.9×10^{-3} mol L^{-1}, pH 7.5 and KNO_3 0.1 mol L^{-1}
458 (same concentration conditions as in Figure 3) .

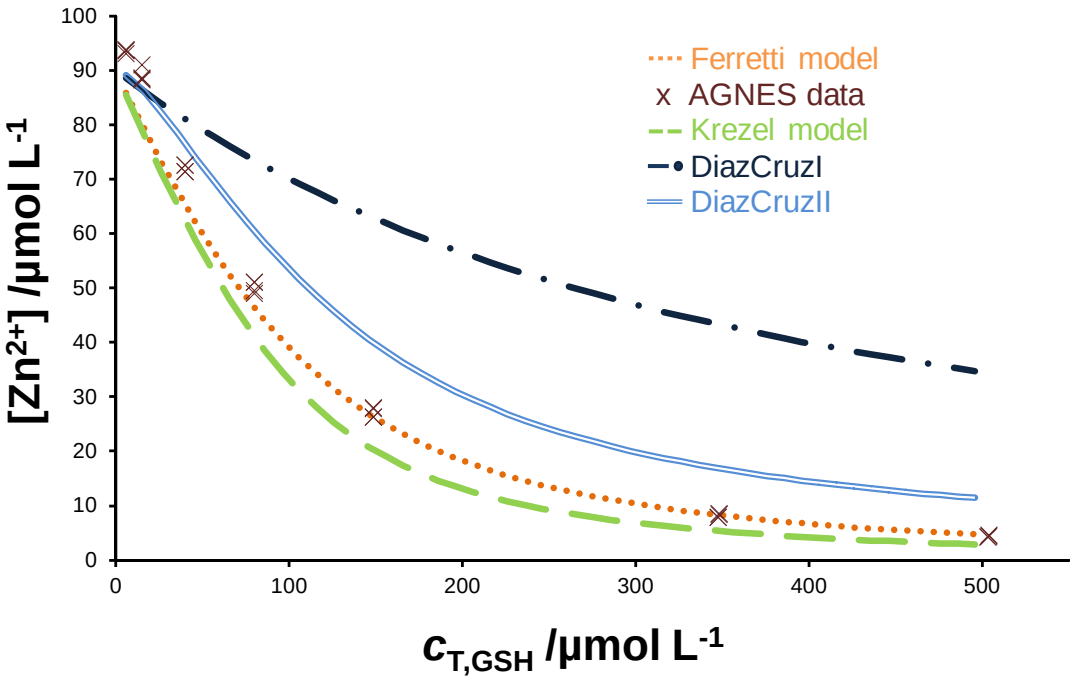

Figure SI-3. $[Zn^{2+}]$ vs $c_{T,GSH}$ added to a solution where $c_{T,Zn}$= 1×10^{-4} mol L^{-1}, pH 7.5 (10^{-2} mol L^{-1} EPPS) and KNO_3 0.1 mol L^{-1}. Brown cross marker corresponds to two replicates of AGNES measurements. Theoretical computations: green dashed line stand for Krezel model, orange dotted line for Ferretti model, dark blue dashed dotted line for DiazCruzI model and double blue line for DiazCruzII model.